

See discussions, stats, and author profiles for this publication at: <https://www.researchgate.net/publication/372552326>

# Glass-LTCC-Interposer, a New Plattform for HF-Applications

Conference Paper · June 2023

DOI: 10.23919/NordPac58023.2023.10186223

CITATIONS

2

READS

364

3 authors:



**Mahsa Mozafari Kaltwasser**

Technische Universität Ilmenau

29 PUBLICATIONS 241 CITATIONS

SEE PROFILE



**Alexander Schulz**

Technische Universität Ilmenau

31 PUBLICATIONS 158 CITATIONS

SEE PROFILE



**Jens Mueller**

Technische Universität Ilmenau

261 PUBLICATIONS 2,050 CITATIONS

SEE PROFILE

# Glass-LTCC-Interposer, a New Plattform for HF-Applications

Mahsa Kaltwasser\*, Alexander Schulz\*, Jens Müller\*

\* Electronics Technology Group

Technische Universität Ilmenau, Gustav-Kirchhoff-Str. 1, 98693 Ilmenau

Email: mahsa.kaltwasser@tu-ilmenau.de

**Abstract—** This publication introduces a new interposer made from a thin glass substrate and a multilayer LTCC compound. Combination of these two material classes into an interposer substrate enables the application of thin-film and thick-film technology in one substrate. In this study thin (100-200  $\mu\text{m}$ ) Borosilicate glass AF45® is applied. The glass substrate includes through glass vias, filled with Au-paste to provide the electrical connection from the glass surface to the underlying electrical structures on the LTCC uppermost layer. The multilayer LTCC green tapes DuPont™ 9K7 are prepared with ground structures on the uppermost layer. After the final lamination of the LTCC-multilayers to the glass, a sintering step causes the mechanical joint of the two materials as an interposer substrate. To demonstrate the Glass-LTCC-Interposer for HF-applications, microstrip line, coplanar waveguide and ring resonator were simulated, designed and fabricated. For the fabrication of fine lines and spaces, the semi-additive technology applying Au-resinate paste in combination with Au-galvanic deposition was utilized. Finally, the realized structures were characterized up to 60 GHz. The HF-investigations of the realized structures on the glass-LTCC-interposer confirm the accuracy of this structuring method. Furthermore, these investigations approve the new interposer as a proper substrate for HF-applications.

**Keywords—** glass-LTCC-interposer; Au-resinate paste; high-resolution HF-structures

## I. INTRODUCTION

The continuous trend towards more intelligent and complex electronic systems requires more miniaturization and higher integration density of microelectronic circuits. Particularly, fine lines and spaces, high-resolution structures, and edges are the requirements for such highly integrated circuits. In recent years, many advanced technologies have been developed to increase the integration density and to enhance data processing capabilities. Silicon interposer technology is one of these [1]. The thin film capability of the silicon substrate enables the heterogeneous integration of multiple active circuits by means of Through-Silicon Vias (TSV). This minimizes signal propagation time and transmission losses. However, due to relatively high conductivity of Si, the electrical structures have to be isolated from the Si-substrate. Nevertheless, the insertion losses for high frequency structures on Si-interposer are still high. Therefore, alternative materials to Si for interposer applications are urgently required. Glass is an alternative material for use as an interposer in integrated circuit packaging [2; 3]. Furthermore, new perspectives opened up due to glass-specific properties such as optical transparency, tailored thermal expansion coefficient and lower dielectric losses compared to silicon. Available glasses with a wide range of coefficient of

thermal expansion (CTE) allow the reliable connection to the next level of interconnect. Additionally, due to the low electrical conductivity of glass there is no need of electrical isolation of the high frequency structures, which leads to less insertion losses. Furthermore, there are variety of technologies which enable the formation of Through Glass Vias (TGV) like laser drilling [4; 5]. Beyond that the use of glass substrates as an interposer allows the generation of optical elements like waveguides or optical gratings directly in glass material or on the glass surface [2; 6]. This enables the combination of electrical and optical functions in one module. On the other hand, the Low Temperature Cofired Ceramics (LTCC) is known for 3D multilayer-wiring and passive high-frequency component integration capability. The combination of both LTCC and glass in one interposer substrate opens new possibilities for various applications in the field of packaging and microelectronics.

This publication presents the new interposer made of glass and LTCC [7]. Similar to Silicon-on-Ceramic substrate (SiCer) [8; 9], the new glass-LTCC-interposer allows the combination of the thick-film with the thin-film technology in one substrate. Therefore, the combination of both LTCC and glass in one interposer substrate stands out as a convenient platform for high frequency and microwave applications, among others. To demonstrate the Glass-LTCC-Interposer for HF-applications microstrip line, coplanar waveguide and ring resonator were designed, simulated and fabricated on the glass surface of the glass-LTCC-interposer. As Glass-LTCC-Interposer aluminoborosilicate glass, AF45® and LTCC-tape 9K7 were applied. To realize the mentioned structures, fine lines and spaces on the glass substrate, a potential and cost-efficient approach is the combination of the thick-film screen printing with the thin-film high resolution photolithography. Special thin-printing pastes, so-called resinate pastes, can be used for this purpose [10; 11]. Resinate pastes consist of metal-organic precious metals dissolved in aromatic oils (metal content 10 - 22 wt%). These pastes can be applied to the glass using full area screen printing. The thickness of the sintered resinate layer is between 0.1 - 1  $\mu\text{m}$ . A sintered resinate layer can be structured by photolithography either directly (if the layer thickness is sufficient) or defined structures can be reinforced to the desired thickness by electroplating. In the latter case, the thin resinate layer, which serves as adhesion layer and plating base, is finally removed by a flash etching step. Finally, the HF-measurements up to 67 GHz using a network analyzer give proofs about the quality of the applied semi-additive structuring technology. Furthermore, conclusions can be achieved from the high

frequency investigations about the glass-LTCC-interposer for HF applications.

## II. GLASS-LTCC-INTERPOSER, FABRICATION

To fabricate the Glass-LTCC-interposer, DuPont Green Tape 9K7 [12] and the Schott alkali-free borosilicate glass AF45 are prepared separately. In this study, 9K7 tape system, which is designed for high frequency applications, is chosen due to its low loss, high dielectric constant and high quality factor  $Q$ . Additionally, the Coefficient of Thermal Expansion, CTE, of the 9K7 tape is in the same range of the one for the glass AF45. Similar CTE of the both material systems is significant for the fabrication of the glass-LTCC-interposer to prevent the mismatches and formation of cracks. For this study, six layers of DuPont 9K7 tapes were applied. After cutting the tapes in 50 mm x 50 mm dimension and preparation of the double tapes (3x) through an isostatic pre-lamination step (100 bar and 70 °C), the tempering step is carried out. The preparation of double tapes reduces the shrinkage caused by detaching the LTCC-tape from the carrier foil. The detaching of the carrier foil occurs before the tempering step. The ground structures, shown in Fig. 1, are realized on the uppermost layer of the LTCC utilizing screen printing method. Subsequently, the three prepared double layers are stacked to one substrate by means of an isostatic lamination step (210 bar at 70 °C).

To enhance the signal propagation from the outer surface of the glass with the HF-structures to the ground layer on the uppermost layer of the LTCC-stack, through glass vias (TGV) are generated in the glass. The TGV with a diameter of 150  $\mu\text{m}$  in 200  $\mu\text{m}$  thin Borosilicate glass AF45 are created using a pico-second laser. Subsequently, the TGV are filled by means of screen printing method using the DuPont Au-through-hole conductor paste TH035. This paste is formulated for minimal shrinkage by the sintering. Therefore, it suites for filling the vias in glass. Fig. 1(B) shows the TGV after sintering and polishing the glass surface.

In order to fabricate an interposer substrate out of Glass and LTCC, the separately prepared glass and LTCC-stack, as mentioned before, are laminated together via an isostatic laminator. A pressure of 210 bar and a temperature of 70 °C is applied for this purpose. Utilizing an isostatic press in every step of the fabrication of the glass-LTCC-interposer is essential to minimize the shrinkage in x- and y-direction. Since the glass material at lower temperatures (<600 °C) is rigid and cannot follow the shrinkage of the LTCC tape, it is significant to avoid the shrinkage. Furthermore, a layer of release tape (500  $\mu\text{m}$  thick) is laminated on the backside of the LTCC-stack in the last lamination step to support the LTCC-tapes from x-y-shrinkage during the lamination and sintering step of the glass-LTCC-interposer. This minimizes the probability of the formation of cracks in glass-LTCC-interposer, especially during the sintering process. The final mechanical joint of the two materials to an interposer is reached in a pressure assisted sintering process. Applying the laminated release tape on LTCC in combination with pressure assisted sintering causes a constrained sintering process. The sintering occurred in a box furnace under air atmosphere. Although, the sintering process of the glass-LTCC-interposer needs some attention. In contrast to the other glass-ceramic LTCC tapes, 9K7 is composed of crystallizable glass,

which builds crystalline phases during the sintering process. These crystalline phases cause the reduction of the dielectric losses [13]. Since the densification of the 9K7 tape is not caused by viscous flow of the glass parts but rather by the crystalline phases, the strain/stress force is high during the sintering step. On the other hand, the CTE of the glass AF45 is  $4.5 \times 10^{-6}/\text{K}$  for temperatures below 300 °C [14]. The CTE of AF45 reduces up to  $3.9 \times 10^{-6}/\text{K}$  by higher temperatures (600 °C) according to the dilatometry investigations. The dominant crystallization behavior of the 9K7 tape and the variation of the CTE of the glass AF45 by higher temperatures should be considered by choosing a proper sintering profile. We used a heating rate of 2.5 °C/min since the shrinkage by lower heating rates is lower [13]. Furthermore, the dielectric constant by this heating rate is ca. 6.8 (at 9 GHz) [15]. Lower ramp rate results in 9K7 to not fully dense material, which leads in lower dielectric constant. The quality factor  $Q$  remains similar by heating rates higher than 2.5 °C/min [13]. The peak-temperature was chosen at 850 °C according to softening temperature of the glass AF45 at 883 °C. The dwell-time was 180 min. The longer dwell-time ensures the saturation of the crystallization. Additionally, the dielectric losses is minimized by higher dwell-time [13; 16].

To avoid the mechanical joint of the glass to the setter plate during the sintering process a release tape is applied at interface glass-setter plate during the sintering step. The release tape causes a high roughness on the glass surface due to the applied pressure by sintering. However, in order to realize fine lines and spaces on the glass surface employing lithography, the glass surface should be polished. Therefore, a polishing step on the glass side of the interposer substrate is employed. First, an  $\text{Al}_2\text{O}_3$  slurry with a grain size of 9  $\mu\text{m}$  was applied to lapp the glass surface to the desired thickness 90  $\mu\text{m}$ . Subsequently, a cerium oxide slurry with a 3  $\mu\text{m}$  grain size followed by a diamond slurry (grain size: 1  $\mu\text{m}$ ) was utilized to polish the surface. The reached roughness on the glass surface after the polishing is ca. 0.005  $\mu\text{m}$  ( $R_a$ ).

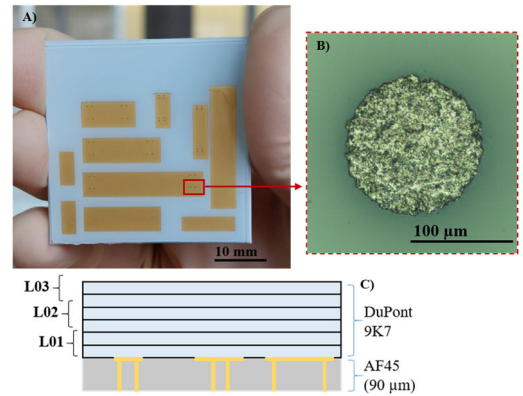


Fig. 1. (A) Glass-LTCC-interposer AF45-9K7 after sintering and polishing the glass surface. The Au-ground structures at the interface glass-LTCC are to observe through the glass. (B) Trough glass via filled with gold. The Au-surface is on the same level as the polished glass surface. (C) The schematic drawing of the cross section of the AF45-9K7-interposer demonstrates the ground structures and the TGVs.

### A. Simulation

To determine the proper dimensions of the different HF-structures on the glass-LTCC-interposer AF45-9K7, simulations with the software SONNET were performed. This study focuses on three different HF-structures, microstrip line, coplanar waveguide and ring resonator. The ground layer is realized on the uppermost LTCC-layer at the interface glass-LTCC, as shown in Fig. 1. The simulation was run for high frequency environments up to 60 GHz. The thickness of the glass layer was considered as 90  $\mu\text{m}$  and the thickness of Au-metal layer as 7  $\mu\text{m}$ . The dielectric constant  $\epsilon_r$  of the glass AF45 and the DuPont tape 9K7 are 6.2 and 7.1, respectively. The dielectric constant of the simulated system was kept at 6.2, since the ground layer is realized at the glass-LTCC interface. Table 1 summarizes the various parameters of the different simulated structures.

TABLE I. SIMULATION VALUES

	Simulation values for HF-structures on AF45-9K7-interposer		
	Microstrip Line	Coplanar Waveguide	Ring Resonator
Value	W: 132 $\mu\text{m}$	W: 99 $\mu\text{m}$ S: 30 $\mu\text{m}$	W: 132 $\mu\text{m}$ G: 50 $\mu\text{m}$ R <sub>i</sub> : 1680 $\mu\text{m}$ R <sub>o</sub> : 1850 $\mu\text{m}$

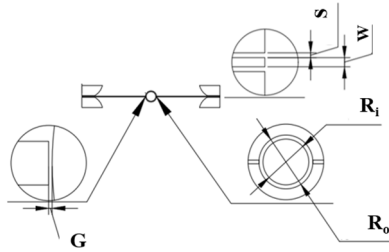


Fig. 2. Schematic drawing of the ring resonator indicating the different dimensions of the HF-structures. The simulated values are listed in table I.

### B. Realization of simulated structures

In order to realize the simulated HF-structures with gold on AF45-9K7-interposer, a semi-additive technology utilizing Au-resinate paste in combination with Au-electroplating is applied. Since a relatively thick Au-layer of about 7  $\mu\text{m}$  is demanded for proper signal propagation, employing the Au-resinate paste and Au-galvanic deposition is much cost-efficient than thin-film technology deposition methods like sputtering or evaporation. The resinate pastes are made of metal-organic compounds dissolved in organic suspension and flux. These pastes can be applied to achieve a homogenous thin metal layer utilizing screen-printing technique. Since the metal amount in the resinate pastes are less than 22% wt%, the electrical conductivity of the printed thin layer is poor. Therefore, reinforcing the thin screen-printed resinate layer by electroplating to the desired thickness is a possible route to improve the electrical properties of this layer. This study uses the Au-resinate paste RP 181208 (Heraeus) with a gold amount of 15% (wt%) and a viscosity of

6.5-8.5 Pas. The Au-resinate paste is applied to the polished glass surface of the AF45-9K7-interposer using a screen with 200 mesh and 15  $\mu\text{m}$  thick emulsion. After the sintering, the Au-layer has a thickness of ca. 300 nm, measured by X-ray fluorescence spectroscopy. This thin Au-resinate layer acts as a seed layer for the subsequent Au-galvanic deposition. Before the electroplating step, the simulated HF-structures are defined by a lithography step on the top the Au-resinate layer. Since a final gold thickness of about 7  $\mu\text{m}$  is desired, 10  $\mu\text{m}$  thick photoresist AZ® 10XT is applied. An additional step of descumming was utilized after the development of the resist to ensure that no residue of the resist is remained. The galvanic deposition is carried out in Au-plating electrolyte AURUNA® 558. The pre-experiments showed a homogenous electroplated Au-layer with smaller grain size with a very low current density. Therefore, the electroplating of 7  $\mu\text{m}$  gold layer was succeeded with a current density of 1 A/dm<sup>2</sup> for 12 minutes at 72 °C in this study. Fig. 3 shows the AF45-9K7-interposer after (A) full area screen-printing of the Au-resinate layer and lithography and (B) after the Au-galvanic deposition.

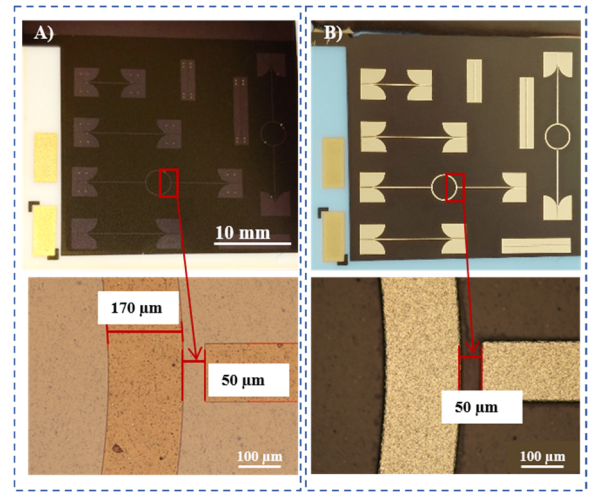


Fig. 3. AF45-9K7-interposer (A) after screen-printing of the Au-resinate paste on the glass surface of the interposer and the lithography step and (B) after the Au-galvanic deposition. The microscopic observations confirm that the simulated dimensions are maintained.

As shown in Fig. 3, an area of 34 x 34 mm<sup>2</sup> was printed with Au-resinate paste. After the Au-galvanic deposition of 12 min a profilometer investigation showed that the Au-thickness is around 9  $\mu\text{m}$ . Since the seed Au-resinate layer should be etched in the next step, it is advantageous that the reinforced structures are thicker than the final value of 7  $\mu\text{m}$ . However, the fine lines between the contact pads have an Au-thickness of about 7  $\mu\text{m}$  directly after the electroplating. This is due to the known electric field distribution over the entire substrate by the galvanic deposition. The small gaps between the structures enhance the non-uniform current distribution on the substrate and therefore a non-uniform coating distribution.



After removing the resist, the 300 nm thick Au-resinate layer, which acted as a seed layer for Au-galvanic deposition, should be removed to complete the fabrication of the HF-structures. The etching of the Au-resinate layer is challenging, since the resinate paste consists of some metals like bismuth or chromium. These metals serve as adhesion agent to the substrate by forming the metal oxides. The commonly used gold etchant  $KI/I_2$  removes the Au-particles but a residue of the other metals remains. Therefore, alternative etchant have been applied to remove this residue. There are two alternatives Au-etchant, KCN and Aqua regia. This study tested both etchant. First, the Au-resinate layer was etched with  $KI/I_2$  for 3 min. The main Au-layer was successfully removed. Fig. 4 demonstrates the results of the etching of the Au-resinate layer with  $KI/I_2$  at room temperature. There are some residue from the resinate paste to observe (Fig 4, D). The dimensions of the realized structures indicated the same dimensions as design  $\pm 5\%$  after this etching step.

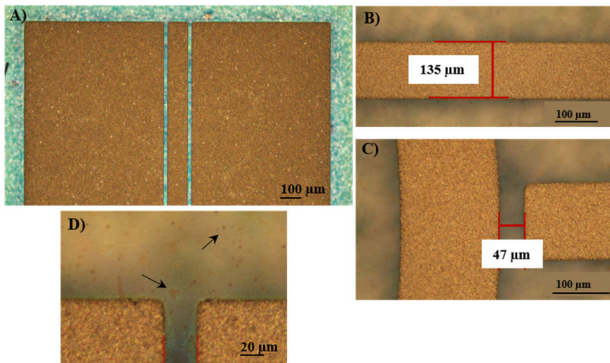


Fig. 4. AF45-9K7-interposer after etching the Au-resinate layer with  $KI/I_2$ . (A) The 300 nm Au-seed layer is not more to observe. The LTCC/ground metalization at interface glass-LTCC is clearly to observe through the glass. (B) and (C) The realized dimensions are the same as design  $\pm 5\%$ . (D) Some residues from the resinate layer is remained.

Second, a diluted solution of the Aqua regia (300 ml  $H_2O$ , 100 ml  $HNO_3$ , and 200 ml  $HCl$ ) was tested at room temperature and 50 °C. At room temperature is the etching rate of the residue very slow. By increasing the temperature, the residue was removed in some seconds and simultaneously the roughness of the galvanic deposited Au-layer increased. Furthermore, it is difficult to control the etching due to the high etching rate by higher temperatures. Therefore, a solution of KCN was tested. A solution of 60 g/l Potassium cyanide, 10 g/l sodium hydroxide, and 5 g/l benzene sulfonic acid was applied. The solution was heated to 60 °C. After 3 minutes, the residue was removed completely. Fig. 5 shows the results of the etching with mentioned KCN-etchant. The resinate residue is removed, the galvanic deposited structures retained its dimensions after this etching step.

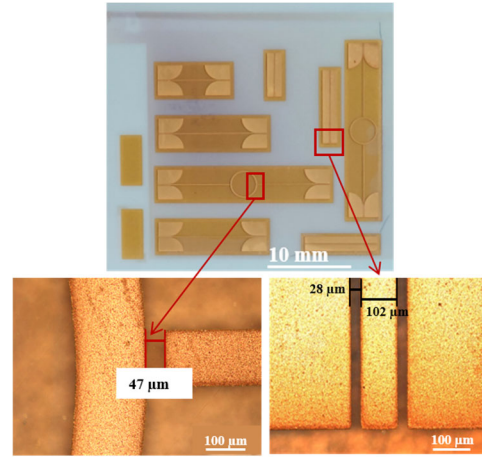


Fig. 5. AF45-9K7-interposer after etching of the Au-resinate seed layer with  $KI/I_2$  and KCN-solution.

### III. HF-INVESTIGATIONS

The realized structures were measured with a network analyzer up to 67 GHz. 250  $\mu m$  pitch GSG measuring tips were applied. The calibration (short-open-load-thru) was performed using a coplanar calibration substrate before measuring the structures. Fig. 6 shows the measurements and the simulation results for the coplanar waveguide (without TGV) with a line length of 10 mm. Both measurement and simulation are in good agreement. The input reflection coefficient  $S_{11}$  is worse for the measured example, which is attributed to the measurement set-up and calibration. The simulation result was achieved by cascading 10 structural simulations using a length of 1 mm in a netlist which could be another source of deviation.

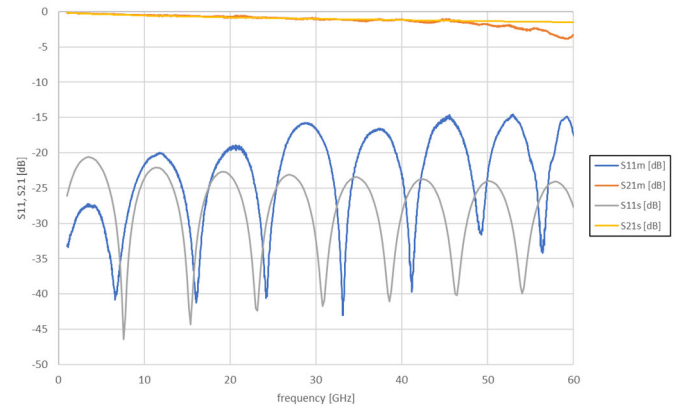


Fig. 6. Network analyzer measurement ( $S_{11m}$ ,  $S_{21m}$ ) and simulation ( $S_{11s}$ ,  $S_{21s}$ ) of the coplanar waveguide with a length of 10 mm. The dimension of this coplanar waveguide is given in table 1.

Fig. 6 demonstrates an approximately 1.8 dB insertion loss @50 GHz. The attenuation per unit line length at this frequency is 1.8 dB/cm. This confirms the HF-compatibility of the glass-LTCC-interposer, AF45-9K7, for the applications up to 40 GHz. For higher frequencies, a better fine-tuning of the design is needed.

The ring resonator (Fig. 5, horizontal resonator) shows the first resonance @13.26 GHz with a quality factor  $Q$  of 74. The

calculated effective permittivity is 4.16 and the attenuation per unit line length at this frequency is 0.32 dB/cm. The other ring resonator (Fig.5, vertical resonator) features almost the same values; first resonance @13.35 GHz with a loaded quality factor of 70. Due to similar values for both ring resonators, it can be concluded that there is isotropic dielectric behavior for this interposer material. These results, especially the quality factor are almost comparable to a similar study of a ring resonator made of copper (thickness 6  $\mu\text{m}$ ) on 100  $\mu\text{m}$  thin glass Schott AF32\_eco ( $\epsilon_r$ : 5.1) with a quality factor of 68 @24 GHz [17].

Some of the designed structures containing TGVs showed an unexpected response with self-resonant effects. An example of such a behavior is shown in Fig. 7 for the microstrip line with TGVs in the grounding pads. The TGVs are combined with a via-free radial stub ground transition design leading to a resonance @16.2 GHz. The spacing of the TGVs is equal to half the wavelength at the resonant frequency.

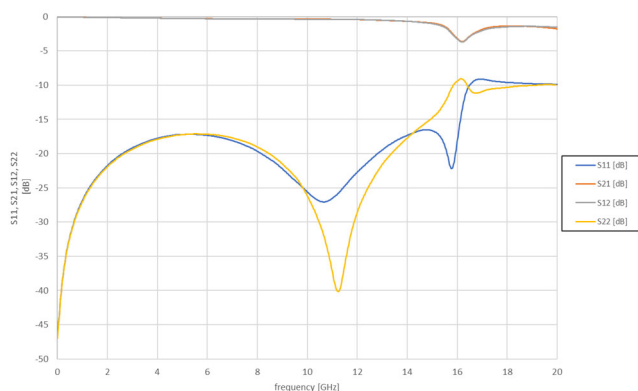


Fig. 7. Measured S-parameters of the microstrip line with a length of 10 mm. The dimension of this microstrip line is given in table 1.

In conclusion, we have shown that the new interposer made from the thin glass AF45 and the LTCC tape DuPont 9K7 is a potential material for HF-applications up to 40 GHz. An optimization of TGVs placement and ground contact pads is required to enhance the HF-properties of the shown structures for frequencies higher than 40 GHz. Additionally, the interposer opens a route to combine the advantages of thin- and thick-film technology in one substrate which enables the realization of fine lines and spaces at reduced costs. The metallization method utilizing the semi-additive technology applying the cost-efficient Au-resinate layer in combination with Au-galvanic deposition was evaluated as a promising technique for fine structuring on glass-LTCC-interposer. A big advantage of the mentioned metallization method is that there is no need of an extra adhesion-promoting layer on top of the glass surface. Furthermore, this publication presents a technique that combines different, already established and well researched technologies

and can therefore be easily transferred to industrial processes and applications.

#### ACKNOWLEDGMENT

This research received financial support through grants from Thüringer Aufbaubank (TAB, Project SPIRIT). We appreciate the support of the Electrochemistry and Electroplating Group and RF and Microwave Research Group of the Technische Universität Ilmenau.

#### REFERENCES

- [1] X. Zhang, J.K. Lin, S. Wickramanayaka, S. Zhang, R. Weerasekera, R. Dutta, K.F. Chang, K.-J. Chui, H.Y. Li, D.S. Wee Ho, *Applied physics reviews* 2 (2015) 021308.
- [2] M. Mirshafiei, J.-P. Bérubé, S. Lessard, R. Vallée, D.V. Plant, *Optics express* 24 (2016) 12375-12384.
- [3] S. Kuramochi, H. Kudo, M. Akazawa, H. Mawatari, M. Tanaka, Y. Fukuoka, *Glass interposer technology advances for high density packaging*, IEEE, 2016, 213-216.
- [4] L.A. Hof, J. Abou Ziki, *Micromachines* 8 (2017) 53.
- [5] A.B. Shorey, R. Lu, *Progress and application of through glass via (TGV) technology*, IEEE, 2016, 1-6.
- [6] A. Desmet, A. Radosavljević, J. Missinne, D. Van Thourhout, G. Van Steenberge, *IEEE Photonics Journal* 13 (2020) 1-12.
- [7] J. Müller, H. Bartsch, M. Fischer, M. Kaltwasser, F. Bechtold, T. Herbst, *Verfahren zur Herstellung eines Glas-Keramik-Verbundsubstrates*, Patent 2022.05.12
- [8] M. Fischer, H.B. de Torres, B. Pawlowski, R. Gade, S. Barth, M. Mach, M. Stubenrauch, M. Hoffmann, J. Müller, *Journal of microelectronics and electronic packaging* 6 (2009) 1-5.
- [9] M. Fischer, T. Mache, B. Pawlowski, D. Schabbel, J. Müller, *Additional Papers and Presentations 2012* (2012) 000158-000161.
- [10] J. Müller, D. Stöpel, T. Mache, A. Schulz, K.-H. Drüe, S. Humbla, M. Hein, *Fineline structuring on LTCC-substrates for 60 GHz line coupled filters*, IEEE, 2011, 1-5.
- [11] D. Stöpel, K.-H. Drüe, S. Humbla, T. Mache, A. Rebs, G. Reppe, A. Schulz, G. Vogt, M. Hein, J. Müller, *Additional Papers and Presentations 2012* (2012) 000607-000612.
- [12] K. Nair, M. McCombs, K. Souders, J. Parisi, K. Hang, D. Nair, S. Beers, *Advances in Electroceramic Materials II* 221 (2010) 213-229.
- [13] S. Dai, *Journal of Materials Science* 47 (2012) 4579-4584.
- [14] T. Meany, S. Gross, N. Jovanovic, A. Arriola, M. Steel, M.J. Withford, *Applied Physics A* 114 (2014) 113-118.
- [15] S. Dai, A. Casias, *Additional Papers and Presentations 2011* (2011) 000302-000305.
- [16] A. Pietrikova, T. Rovensky, J. Durisin, I. Vehec, O. Kovac, *Microelectronics International* 34 (2017) 127-130.
- [17] M. Letz et al., *Attenuation of high frequency signals in structured metallization on glass: Comparing different metallization techniques with 24 GHz, 77 GHz and 100 GHz structures*, 2019 IEEE 69th Electronic Components and Technology Conference (ECTC), IEEE, 2019, pp. 726-732.